

Chirp as Precompensation Factor to Reduce BER on Gaussian and Super Gaussian Pulses in OCDMA System

Mojaiana Synthia¹ and Md. Shipon Ali^{1*}

¹*Electronics & Communication Engineering Discipline, Khulna University,
Khulna- 9208, Bangladesh
Email* : mdshipon.ku@gmail.com*

Abstract

Optical Code Division Multiple Access (OCDMA) is the technique to share a wide bandwidth among a large number of users, OCDMA combines high bandwidth Fiber optic media with flexibility of OCDMA, to provide high-speed connectivity. Multiple Access Interference (MAI) is the main source of performance degradation in OCDMA system. MAI is such a type of interference which caused by multiple cellular users who are using the same frequency allocation at the same time. This is actually a noise which can't be eliminated anyhow from the system. It can be reduced by decreasing the probability of Bit Error Rate (BER). In this paper we have to examine the way in which the probability of BER would be reduced by considering the chirp effect on Gaussian and Super Gaussian pulses within different conditions.

Keywords: Chirp, OCDMA, MAI, BER, APD

1. Introduction

In the OCDMA systems, the low rate base-band signals are mapped into the high rate optical pulse sequences, and transmitted in optical fibers. The duration of optical pulse is generally up to picoseconds or sub picoseconds level. On account of the fiber dispersion effect, the high rate optical pulse propagating along fibers occurs broadening, and results in the signal-to-noise ratio (SNR) of receiver decreasing. So, the fiber dispersion effect is a critical limiting factor of OCDMA systems. Dispersion compensation refers to the process of designing the fiber and compensating elements in the transmission path to keep the total dispersion to a small number. This process controls the overall dispersion of a system by adding optical elements with a suitable amount of dispersion.

2. Methodology

In our analysis, Optical Orthogonal Codes (OOCs) have employed as address sequence codes. Avalanche photodiode (APD) has selected as the system receiver. The effects of APD - shot noise, bulk dark current, surface leakage current, thermal noise current and MAI have considered. The loss of system devices has omitted. The systems performance has evaluated under the assumption of optical signal power, code length and code weight are constant. The numerical results have computed for the practical values of the system parameters below.

Parameters	Values
Code length, F	409
Code weight, K	4
Maximum number of users, N	35
Average APD gain, M	20
Excess noise index, x	0.7
Average bulk dark current, IBD	2 nA

Average surface leakage current, ISL	10 nA
Receiver load resistance, RL	1000 Ω
Extinction ratio, γe	0.05
SMF dispersion, D	18 ps/(km-nm)
Optical signal power, P=KPS	-25 dBm
Receiver noise temperature, T	300 K
Fiber wave length, λ	1.55 μm

3. BER Performance Analysis

At the receiving terminal, the correlation operation between received signal and a replica of the desired user's address code is carried out by optical correlator to achieve decoding. The decoding signal is incident on the APD, the output current Y_1 sampled at time $t = T_b$ can be written as

$$Y_1 = X_1 + I_1 + I_n \dots\dots\dots (3.1)$$

Where,

- X_1 = User's signal current.
- I_1 = Interference signal current offered by MAI.
- I_n = APD noise current.

I_n include shot noise current, bulk dark current, surface leakage current and thermal noise current. We assume that the (F, K, 1) OOCs are selected as user address codes. By the correlation definition of OOCs, each interference user can contribute at most one hit during the correlation time. If v is an integer ($0 \leq v \leq N - 1$) denotes the total number of hits from interference users, the probability density function of v is given by [5]

$$p(v) = \binom{N-1}{v} s^v t^{N-1-v} \dots\dots\dots (3.2)$$

Where,

$$s = K^2/2F,$$

$$t = 1 - s$$

If code length F, code weight K and v are given, the first two terms of equation (3.1) can be determined [7]. We assume that the APD noise current has Gaussian nature. The output photocurrent Y_1 can be regarded as a Gaussian random variable. Its average μ_1 and variance σ_1^2 for bit "1" and "0" are determined. Since the received signal is multiplied by the user address code, *i.e.*, (0, 1) sequence. During the bit "1" interval of the desired signal, photons fall on the APD only during the K mark intervals and are totally blocked during the (F-K) space intervals. During the K chip intervals of the desired signal, the total number of pulses (either marks or spaces) due to N users is KN. Among these KN pulses, there is (K + v) mark pulses with power level $C_d P_s$, and $KN - (K + v)$ space pulses with power level $C_d \gamma_e P_s$

Here,

- C_d represents the effect of SMF dispersion and pulse linear chirp,
- γ_e is the Extinction ratio of APD receiver.

Therefore, μ_1 and σ_1^2 are given by

$$\mu_1 = M(R_0 + P_t^1 + I_{BD}) + I_{SL} \dots\dots\dots (3.3)$$

$$\sigma_1^2 = 2eM^{2+x}(R_0 + P_t^1 + I_{BD})(B_e + 2eI_{SL}B_e + \frac{4K_B T}{R_L} B_e) \dots\dots\dots (3.4)$$

Where,

$$P_t^1 = vC_d P_s + (KN - K - v)C_d \gamma_e P_s \dots\dots\dots (3.5)$$

The C_d is given by [3]

$$C_d = \left[1 + \frac{\gamma(1/2m) C \beta_{2z}}{\gamma(3/2m) T_0^2} + m^2 (1 + C^2) \frac{\gamma \left(\frac{2-1}{2m} \right) \left(\frac{\beta_{2z}}{T_0^2} \right)^2}{\gamma(3/2m)} \right]^2 \dots\dots\dots (3.6)$$

Where,

The exponent x varies between 0 and 1.0 depending on the APD material and structure.

- M = Average APD gain.
- R_0 = Unity gain responsivity.
- e = Electron charge (1.601×10^{-19} C).
- I_{BD} = Average bulk dark current, which is multiplied by the avalanche gain.
- I_{SL} = Average surface leakage current, which is not affected by avalanche gain.
- B_e = Receiver electrical bandwidth.
- K_B = Boltzmann's constant (1.379×10^{-23}).
- T = Receiver noise temperature.
- R_L = Receiver load resistor.

For data bit "0", average μ_0 , variance σ_0^2 of photocurrent Y_1 can be determined in the same way as for data bit "1". In this case, μ_0 and σ_0^2 can be written as:

$$\mu_0 = M(R_0 + P_t^0 + I_{BD}) + I_{SL} \dots\dots\dots (3.7)$$

$$\sigma_0^2 = 2eM^{2+x}(R_0 + P_t^0 + I_{BD})(B_e + 2eI_{SL}B_e + \frac{4K_B T}{R_L} B_e) \dots\dots\dots (3.8)$$

Where,

$$P_t^0 = vC_d P_s + (KN - v)C_d \gamma_e P_s \dots\dots\dots (3.9)$$

For the desired user's data bit "1" or "0", the conditional probability density function of the output photocurrent Y_1 can be expressed as:

$$p_{Y_1} \left(\frac{y}{v}, \text{bit 1} \right) = \frac{1}{\sqrt{2\pi\sigma_1}} \exp \left[\frac{-(y-\mu_1)^2}{2\sigma_1^2} \right] \dots\dots\dots (3.10)$$

$$p_{Y_1} \left(\frac{y}{v}, \text{bit 0} \right) = \frac{1}{\sqrt{2\pi\sigma_0}} \exp \left[\frac{-(y-\mu_0)^2}{2\sigma_0^2} \right] \dots\dots\dots (3.11)$$

For a given threshold level Th , the probability of error for bit "1" and "0" are calculated by

$$\begin{aligned} p_e^{(1)}(v) &= \int_0^{Th} p_{Y_1} \left(\frac{y}{v}, \text{bit 1} \right) dy \\ &= \frac{1}{2} \operatorname{erfc} \left[\frac{\mu_1 - Th}{\sqrt{2}\sigma_1} \right] \dots\dots\dots (3.12) \end{aligned}$$

$$\begin{aligned} p_e^{(0)}(v) &= \int_{Th}^{\infty} p_{Y_1} \left(\frac{y}{v}, \text{bit 0} \right) dy \\ &= \frac{1}{2} \operatorname{erfc} \left[\frac{Th - \mu_0}{\sqrt{2}\sigma_0} \right] \dots\dots\dots (3.13) \end{aligned}$$

The probability of error per bit, depended on the threshold level Th , is defined as:

$$p_e(v) = \frac{1}{2} [p_e^{(1)}(v) + p_e^{(0)}(v)] \dots\dots\dots (3.14)$$

Here, it is assumed that the bit "1" and "0" have the identical probability. To make the above expression achieves minimum value; an optimum threshold level can be obtained,

$$Th = \frac{\mu_1 \sigma_0 + \sigma_0 \sigma_1}{\sigma_0 + \sigma_1} \dots\dots\dots (3.15)$$

The total probability of error P_e per bit is given by

$$p_e = \sum_{v=0}^{N-1} p_e(v) \binom{N-1}{v} s^v t^{N-1-v} \dots\dots\dots (3.16)$$

4. Simulation

In this paper, the system Bit Error Rate (BER) with practical parameters has computed with respect to the number of users by applying the equation (3.16). In numerical calculation, it assumed that OOCs are the address sequence and the InGaAs APD is selected as the system receiver. Primary parameters have taken as in table (Section 2). Here the chirp effect to compensate the dispersion has been accounted from 0 to 2.5. Throughout this computation two curves have set as reference curve. In one condition, data transmission is occurred when there is no chirp and no dispersion effect ($C=0$ and $D=0$). Second reference curve shows the data transmission with a certain dispersion but no chirp effect ($C=0$ and $D=18$ ps/(km-nm)). Figure (4.1) and Figure (4.2) shows the effect of chirp on Gaussian pulses to compensate the dispersion at $Z=5$ km and $Z=10$ km, respectively.

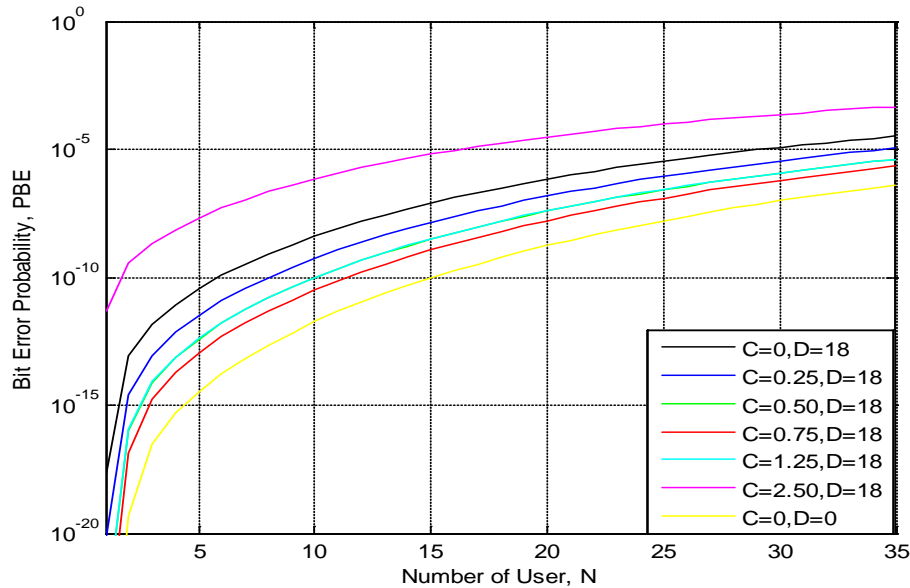


Figure 4.1. Effect of Chirp on Gaussian Pulse at z = 5 km

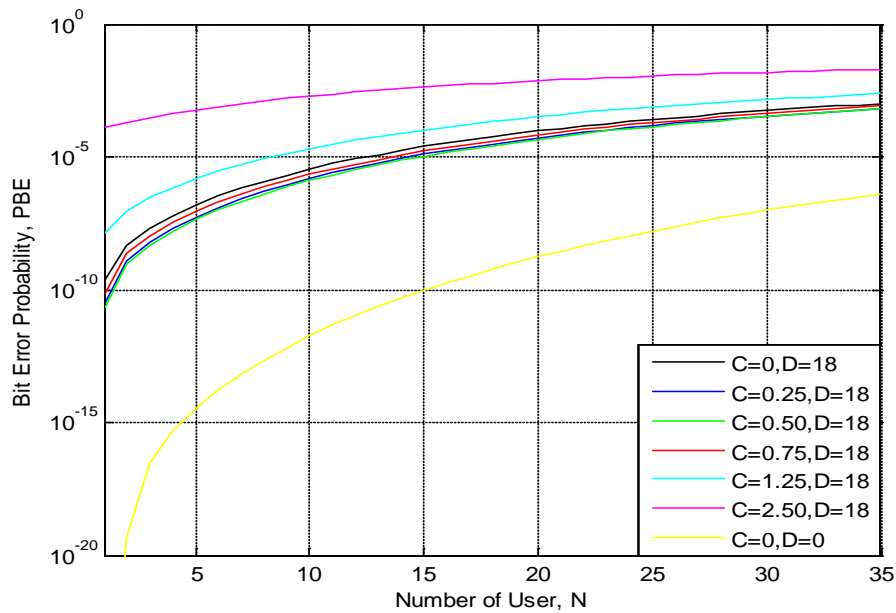


Figure 4.2. Effect of Chirp on Gaussian Pulse at $z = 10$ km

From Figure 4.1 it is clear that a better compensation is achieved due to the chirp effect and the most expected achievement is occurred at a certain value of chirp (here $C=0.75$). Also, from Figure (4.2) it is seen that a little compensation is achieved for long distance data transmission and the chirp value for most compensation shift from 0.75 to 0.50.

Again, Figure 4.3 and Figure 4.4 analyses the effect of chirp on super Gaussian pulses ($m=2$, m is the degree of edge sharpness) to compensate the dispersion at $Z=2$ km and $Z=5$ km, respectively. From these two figures it is observed that for same transmission path, better compensation is achieved for short distance transmission over long distance and the optimum chirp value is different for different length of transmission path. Here, from Figure 4.3 it seems that the compensation is achieved at every value of chirp up to 1.5 and the better achievement occur at $C=0.75$. On the other hand, Figure 4.4 shows a little compensation at value of chirp up to 0.75.

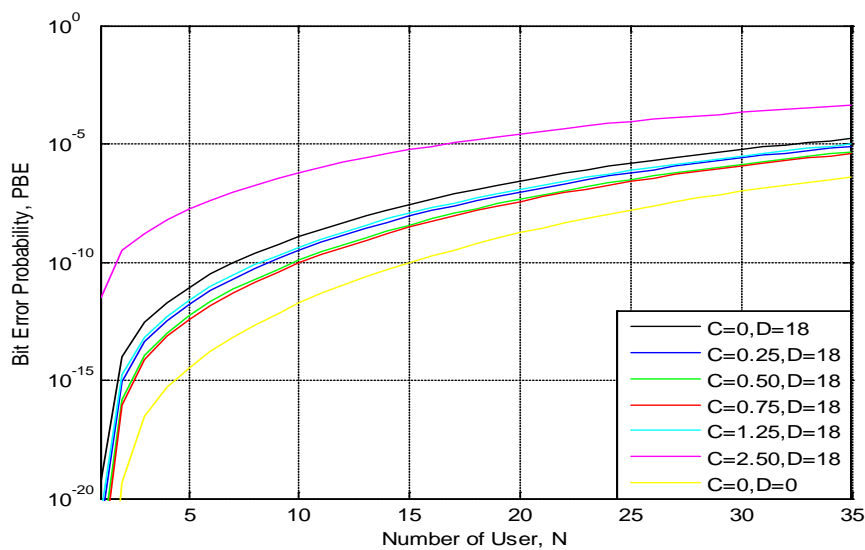


Figure 4.3. Effect of Chirp on Super-Gaussian Pulse ($m=2$) at $z = 2$ km

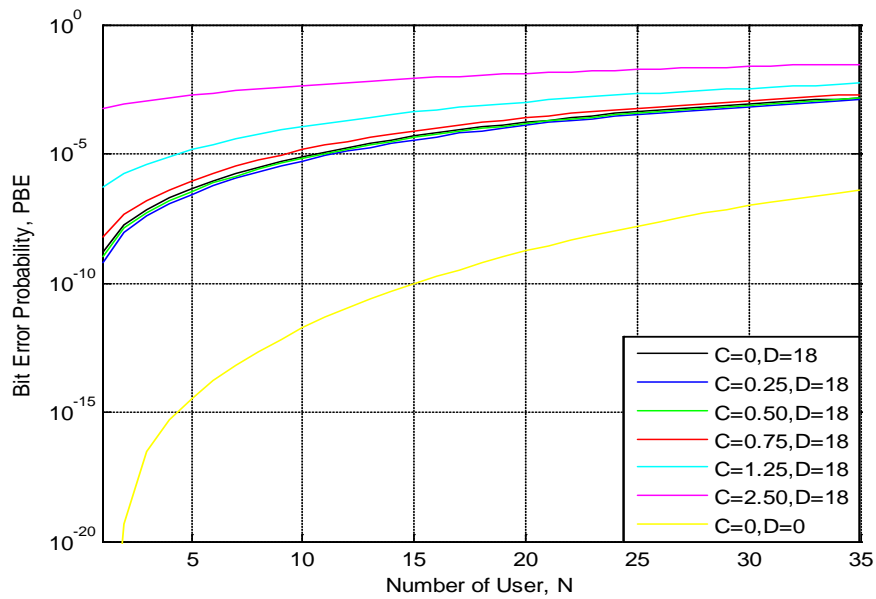


Figure 4.4. Effect of Chirp on Super-Gaussian Pulse ($m=2$) at $z = 5$ km

In addition, Figure 4.5 and Figure 4.6 shows the chirp effect on super Gaussian pulses ($m=5$) to compensate the dispersion at $Z=2$ km and $Z=5$ km, respectively. Here a very little compensation is achieved due to chirp effect. This result completely coincides with previous observations that the less BER occur for short distance transmission than long distance within the same transmission path.

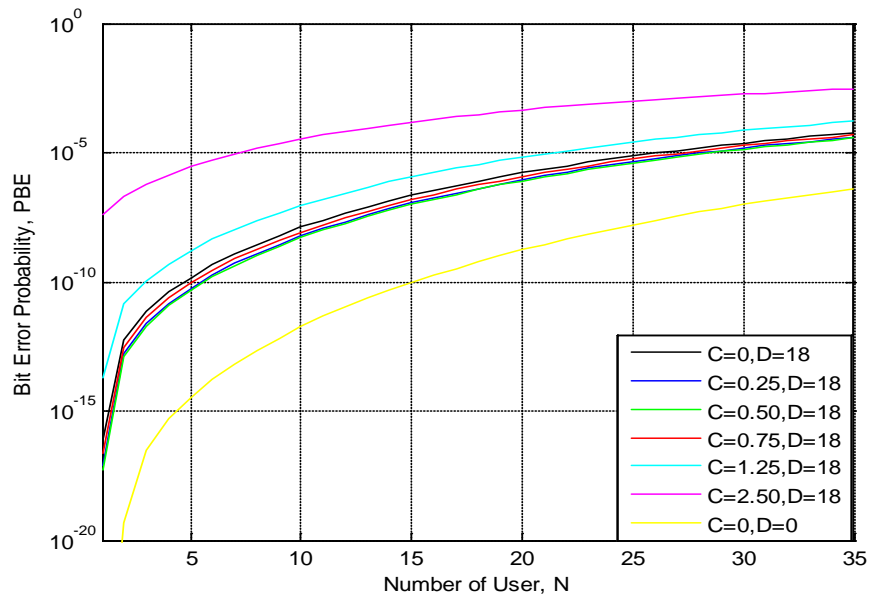


Figure 4.5. Effect of Chirp on Super-Gaussian Pulse ($m=5$) at $z = 2$ km

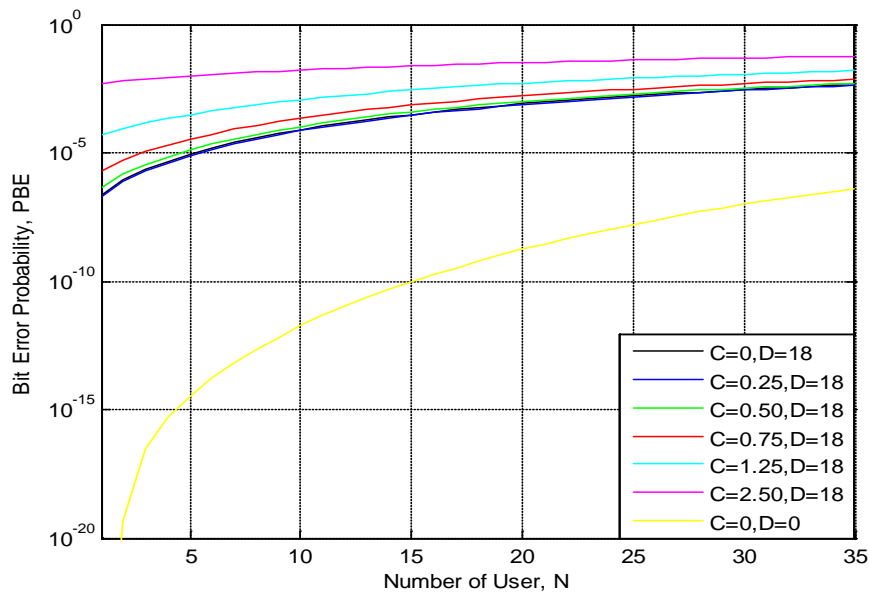


Figure 4.6. Effect of Chirp on Super-Gaussian Pulse (m=5) at z = 5 km

5. Results and Conclusion

Dispersion-induced broadening is sensitive to pulse edge steepness. In general, a pulse with steeper leading and trailing edges broadens more rapidly with propagation simply because such a pulse has a wider spectrum to start with. The differences between the Gaussian and super-Gaussian pulses can be attributed to the steeper leading and trailing edges associated with a super-Gaussian pulse. Whereas the Gaussian pulse maintains its shape during propagation, the super-Gaussian pulse not only broadens at a faster rate but also distorts in shape.

In this paper we have investigated that due to chirp effect for same transmission path and distance a better compensation of pulse dispersion is achieved for Gaussian pulses than the super-Gaussian pulses and the compensation due to chirp effect decreases as “m” increases. We also find that due to chirp effect, better dispersion compensation is achieved for short range of data transmission than the long distance transmission but the maximum compensation in each different condition is achieved for different values of chirp while other parameters remain the same.

References

- [1] J. M. Senior, “Optical Fiber Communications”, 2nd Edition.
- [2] F. R. K. Chung and J. A. Salehi, “Optical orthogonal codes: design, analysis, and applications”, IEEE Trans. Inform. Theory, vol. 35, no. 5, (1989), pp. 595-604
- [3] D. Anderson and M. Lisak, “Opt. Lett”, vol. 11, (1986), pp. 569.
- [4] T. Ohtsuki, “Channel Interference Cancellation Using Electro-Optic Switch and Optical Hardlimiters for Direct-Detection Optical CDMA Systems”, J. Lightwave Technol., vol. 16, no. 4, (1998), pp. 520-526.
- [5] J. A. Salehi, “Code Division Multiple-Access Techniques in Optical Fiber Networks-Part: Fundamental Principles”, IEEE Trans. Commun., vol. 37, no. 8, (1989), pp. 824-833.
- [6] G. Keiser, “Optical Fiber Communications”, Third Edition, The Mc Graw-Hill Companies, Inc., (2000).
- [7] Dr. Nasir and Dr. Gohar, “Optical CDMA – An Introduction”.
- [8] H. M. H. Shalaby, “Chip-Level Detection in Optical Code Division Multiple Access”, J. Lightwave Technol., vol. 16, no. 6, (1998), pp. 1077-1087.
- [9] H. M. Kwon, “Optical Orthogonal Code-Division Multiple Access System-Part: APD Noise and Thermal Noise”, IEEE Trans. Commun., vol. 45, no. 11, (1994), pp. 1426-1433.

- [10] V. K. Jain: "Performance evaluation of optical code division multiple access networks"; J. Optical Commun., vol. 21, no. 3, (2000), pp. 110-115.
- [11] D. Marcuse, "Appl.Opt", vol. 19, (1980), pp. 1653.
- [12] T. Ohtsuki: "Performance analysis of direct detection optical asynchronous CDMA systems with double optical hard limiters", J. Light wave Technol., vol. 15, no. 3, (1997), pp. 452-457.
- [13] A. Yariv, "Optical Electronics in Modern Communications"; Fifth Edition, Oxford University Press, Inc., (1997).
- [14] G. P. Agrawal, "Fiber-Optic Communication Systems", Wiley, NewYork, (1997), Chap.2
- [15] Core Technology Demonstration on Ultra Fast Wavelength Hopping OCDMA - E. Chen, H. Chen & Y. Tang